

Generic Contrast Agents

Our portfolio is growing to serve you better. Now you have a *choice*.



[VIEW CATALOG](#)

AJNR

Multiple Sclerosis: Comparison of Trace Apparent Diffusion Coefficients with MR Enhancement Pattern of Lesions

Sudipta Roychowdhury, Joseph A. Maldjian and Robert I. Grossman

This information is current as of May 7, 2025.

AJNR Am J Neuroradiol 2000, 21 (5) 869-874
<http://www.ajnr.org/content/21/5/869>

Multiple Sclerosis: Comparison of Trace Apparent Diffusion Coefficients with MR Enhancement Pattern of Lesions

Sudipta Roychowdhury, Joseph A. Maldjian, and Robert I. Grossman

BACKGROUND AND PURPOSE: Diffusion-weighted MR imaging and the trace apparent diffusion coefficient (ADC) provide important structural information about tissues. The purpose of this study was to investigate the relationship between trace ADC values and the enhancement pattern of multiple sclerosis (MS) lesions.

METHODS: Ninety-six lesions, identified in 24 patients with MS, were characterized by their enhancement pattern on contrast-enhanced T1-weighted MR images. There were 57 nonenhancing lesions (NELs), 28 homogeneously enhancing lesions (HELs), and 11 ring-enhancing lesions (RELs). The trace ADC means for each type of lesion and for normal-appearing white matter (NAWM) were calculated and compared using Student's *t*-test.

RESULTS: The mean trace ADC values for HELs (mean, $7.7 \times 10^{-10} \text{ m}^2\text{s}^{-1}$; SD, $1.4 \times 10^{-10} \text{ m}^2\text{s}^{-1}$) were less than those for RELs (mean, $1.2 \times 10^{-9} \text{ m}^2\text{s}^{-1}$; SD, $3.5 \times 10^{-10} \text{ m}^2\text{s}^{-1}$) and NELs (mean, $1.3 \times 10^{-9} \text{ m}^2\text{s}^{-1}$; SD, $2.6 \times 10^{-10} \text{ m}^2\text{s}^{-1}$). There was a significant difference between the mean trace ADC values of HELs and RELs as well as between those for HELs and NELs. There was also a significant difference in the mean trace ADC values between all lesion types and NAWM (mean, $6.9 \times 10^{-10} \text{ m}^2\text{s}^{-1}$; SD, $5.0 \times 10^{-11} \text{ m}^2\text{s}^{-1}$).

CONCLUSION: We found a predictable relationship between mean trace ADC and the pattern of enhancement in MS lesions, corresponding to reported histopathologic differences in myelination between lesion types and magnetization transfer ratios.

The histopathologic characteristics of multiple sclerosis (MS) lesions differ according to the pattern of enhancement on MR images (1, 2). Nonenhancing lesions (NELs) histologically have scarring with minimal inflammation and variable myelin loss, ranging from mild to severe. Homogeneously enhancing lesions (HELs) have prominent inflammation but only mild demyelination. Ring-enhancing lesions (RELs) have complete central myelin loss with peripheral inflammation. The magnetization transfer ratios (MTRs) have been studied for the enhancement pattern of MS lesions (3). HELs had a higher mean MTR than did NELs and RELs. This is probably related to the greater degree of

myelin preservation in HELs as compared with RELs or NELs. Hypointense lesions on T1-weighted spin-echo MR images, which can be seen in NELs as well as RELs, are associated with severe tissue destruction (4).

Diffusion-weighted MR imaging is an important tool in the evaluation of the random molecular motion of water protons (5–7), and there has been great interest in the use of this technique for the study of stroke (6, 8–12). The trace apparent diffusion coefficient (ADC) provides a rotationally invariant measurement of the total diffusion of water within a tissue (7–12). Diffusion-weighted MR imaging offers an opportunity to evaluate the structural characteristics of tissues. White matter is composed of highly organized myelinated axons that create an anisotropic restriction of water diffusion (10, 13–17). Therefore, any process that results in changes in the structural elements of tissue may also affect its diffusion characteristics.

Early investigators used diffusion-weighted MR imaging in the evaluation of MS (18–23). These studies showed increases in ADC values in MS lesions and perhaps also in the ADC values of normal-appearing white matter (NAWM) of MS patients (18–21). Although the reason for the increase

Received July 30, 1999; accepted after revision December 6.

From the Department of Radiology, Hospital of the University of Pennsylvania, Philadelphia (S.R., J.A.M., R.I.G.); and the Department of Radiology, University of Medicine and Dentistry of New Jersey, New Brunswick (S.R.).

Supported by grants NS29029, NS29020-09, and 5M01-RR00040-34 from the National Institutes of Health.

Address reprint requests to Joseph A. Maldjian, MD, Department of Radiology, Neuroradiology Section, Hospital of the University of Pennsylvania, Ground Floor Founders Building, 3400 Spruce St, Philadelphia, PA 19104.

in ADC is not known, it is believed to be related to the disruption of myelin, leading to an increased extracellular space (18–21).

In this study, we compared the trace ADC measurements of NELs, HELs, RELs, and NAWM in MS patients to determine whether there is a pattern that corresponds to the MR findings and that accounts for what is known about the histopathologic characteristics and MTRs of the different lesion types.

Methods

During a period of 2 years (1997–1999), we identified 24 patients with MS in whom enhancing lesions were found on MR images. Most of the patients were in an MS cohort entered in a National Institutes of Health study consisting of serial MR examinations. In all patients, MS was diagnosed by means of the Poser criteria (24). The study group comprised 17 women and seven men with a mean age of 41 years. All lesion characterization and analyses were performed by one neuroradiologist who was not blinded to patient data or imaging findings. Lesions analyzed were at least 5 mm in diameter and were detected on long-TR/long-TE sequences. Lesions were said to be enhanced if they were significantly hyperintense relative to white matter on T1-weighted images after intravenous administration of gadopentetate dimeglumine (0.1 mmol/kg, up to maximum of 20 mL). RELs were differentiated from HELs by virtue of having a central nonenhancing region and a peripheral

enhancing rim. Fifty-seven NELs (Fig 1), 28 HELs (Fig 2), and 11 RELs (Fig 1) were evaluated.

MR examinations were performed on a 1.5-T clinical imager equipped with an Echospeed gradient system for echo-planar imaging. Sagittal T1-weighted images were obtained with the following parameters: 500–700/17–30/1 (TR/TE/excitations), 5-mm-thick sections, 256×192 matrix, and a 22-cm field of view (FOV). For axial fast spin-echo (FSE) T2-weighted images, the parameters were as follows: 2500–4000/80–110/1, 5-mm-thick sections, 256×192 matrix, and 22-cm FOV. Axial contrast-enhanced T1-weighted images were acquired with the following parameters: 500–700/20–40/1, 3- or 5-mm-thick sections, 256×192 matrix, and 22-cm FOV. Diffusion-weighted imaging was performed prior to contrast administration in all cases and used a spin-echo echo-planar sequence with parameters as follows: 4000/125, 128×128 matrix, 24-cm FOV, and b value of 1000 s/mm². The diffusion gradients were applied sequentially in three orthogonal directions to generate three sets of axial diffusion-weighted images (S_x , S_y , and S_z) in addition to a baseline image (S_0), with no diffusion gradients. The diffusion-weighted images were transferred to a workstation for off-line processing using software developed in IDL (Research Systems Inc, Boulder, CO). Isotropic diffusion-weighted images were calculated using the relationship

$$S = \text{cube root } (S_x * S_y * S_z).$$

Diffusion trace maps were computed from the isotropic diffusion image and the baseline image on a pixel-by-pixel basis using the relationship

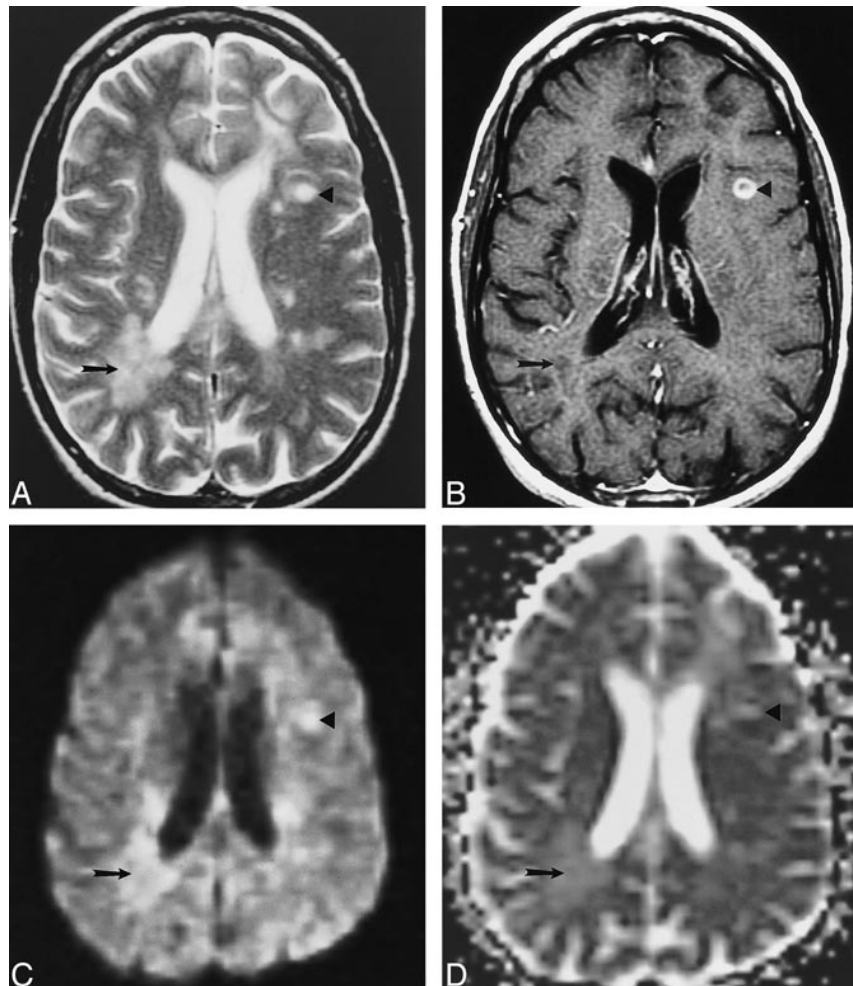


FIG 1. Examples of an NEL and an REL in a patient with MS.

A–D, Axial T2-weighted image (4000/110/1) (A), contrast-enhanced T1-weighted image (500/20/1) (B), isotropic diffusion-weighted image (4000/125/1) (C), and trace ADC map (D) show a T1-weighted NEL (arrow) and a T1-weighted REL (arrowhead). Both lesions show increased diffusion on the trace ADC map.

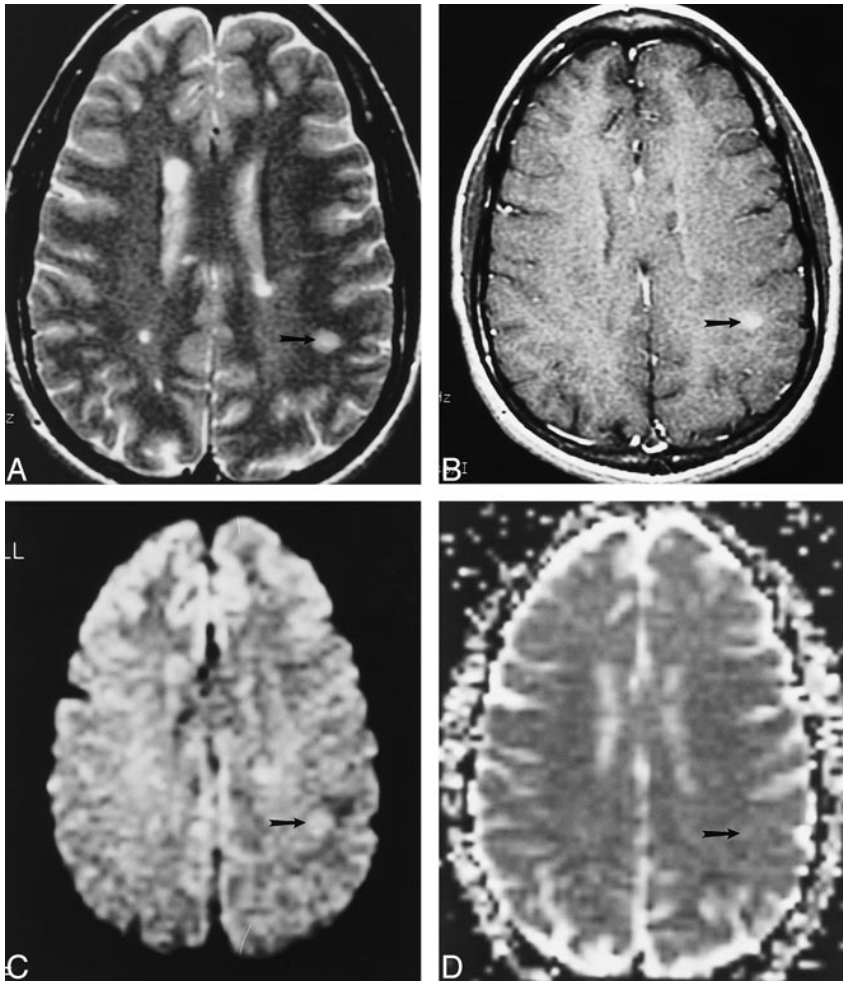


FIG 2. Example of an HEL in a patient with MS.

A–D, Axial T2-weighted image (4000/110/1) (A), contrast-enhanced T1-weighted image (500/20/1) (B), isotropic diffusion-weighted image (4000/125/1) (C), and trace ADC map (D) show a T1-weighted HEL (arrow), which shows increased diffusion on the trace ADC map.

$$S = S_0 e^{-(bD)}$$

in which S is the isotropic diffusion-weighted signal, S_0 is the baseline signal intensity without diffusion gradients, D is the average trace, and b is the gradient attenuation factor. The trace ADC is a rotationally invariant measurement of the amount of total diffusion within a tissue (7, 12, 13, 16, 25, 26).

Regions of interest (ROIs) were drawn directly on the baseline S_0 images of the diffusion MR sequence. These were determined from careful visual comparison between the T2-weighted, contrast-enhanced T1-weighted, and S_0 baseline images. All enhancing lesions were easily identified on the FSE T2-weighted images, and all lesions seen on the FSE T2-weighted sequences were easily identified on the corresponding baseline image. The ROIs placed on the baseline image were applied to the trace maps to obtain the corresponding trace ADC values. Trace ADC measurements were recorded with the ROI placed around the entire lesion in the case of NELs and HELs. For RELs, the ROI was placed within the nonenhancing center of the lesion. The mean of three trace ADC measurements was recorded for each lesion. In every patient, the trace ADC was obtained in the NAWM in two bilateral areas for a total of four measurements. These values were compared with the normal white matter (NWM) ADC values, which we have compiled for healthy volunteers at our institution.

Statistical significance was calculated for the trace ADC of each type of lesion and for NAWM using a two-tailed Student's t -test. The mean trace ADC for each lesion type (NEL, HEL, and REL) was compared with the other lesions and with the mean trace ADC of NAWM in the 24 patients. The mean

trace ADC of NAWM was compared with that of NWM in five healthy volunteers.

Results

The mean trace ADC measurements and SDs for NELs, HELs, RELs, and NAWM are shown in the Table. All three types of MS lesions had higher mean trace ADCs than did NAWM. There was a significant difference between the mean trace ADCs of each lesion type compared with NAWM: NELs and NAWM ($P < .0001$), HELs and NAWM ($P < .01$), and RELs and NAWM ($P < .0001$). There was also a significant difference between the mean trace ADCs of HELs and RELs ($P < .01$) as well as between HELs and NELs ($P < .0001$). There was no significant difference between the mean trace ADCs of NELs and RELs ($P = .63$). The trace ADC measurements for NWM in a group of five healthy patients (mean, $6.7 \times 10^{-10} \text{ m}^2\text{s}^{-1}$; SD, $9.2 \times 10^{-11} \text{ m}^2\text{s}^{-1}$) did not significantly differ from those of NAWM (mean, $6.9 \times 10^{-10} \text{ m}^2\text{s}^{-1}$; SD, $5.4 \times 10^{-11} \text{ m}^2\text{s}^{-1}$) in the 24 MS patients ($P = .18$).

During serial MR imaging, two lesions were identified that showed changes in enhancement pattern over time. In one patient, an HEL (trace ADC,

Summary of trace apparent diffusion coefficient (ADC) measurements

Lesion Type	No.	Mean Trace ADC ($10^{-10} \text{ m}^2 \text{ s}^{-1}$)	SD (%)	Maximum ($10^{-10} \text{ m}^2 \text{ s}^{-1}$)	Minimum ($10^{-10} \text{ m}^2 \text{ s}^{-1}$)
Nonenhancing	57	12.5	21	20.0	6.5
Homogeneously enhancing	28	7.7	19	9.9	4.1
Ring-enhancing	11	11.9	30	21.4	9.0
Normal-appearing white matter	96	6.9	8	8.5	5.8

$7.5 \times 10^{-10} \text{ m}^2 \text{ s}^{-1}$) became an NEL (trace ADC, $9.7 \times 10^{-10} \text{ m}^2 \text{ s}^{-1}$) after a 9-month follow-up period. In another patient, an REL (trace ADC, $2.1 \times 10^{-9} \text{ m}^2 \text{ s}^{-1}$) became an NEL (trace ADC, $1.8 \times 10^{-9} \text{ m}^2 \text{ s}^{-1}$) over a period of 11 months.

Discussion

The initial event in the development of an MS lesion may be the disruption of the blood-brain barrier (BBB), which is associated with a prominent inflammatory process (1, 29, 30). Antigen-specific T cells enter the CNS and begin a cytokine cascade, which activates endothelial cells and mediates the opening of the BBB (1). The process continues with the recruitment of additional cells with amplification of the inflammatory response (1, 27, 28). Contrast enhancement on MR images reflects this transient disruption of the BBB with extravasation of contrast material into the brain parenchyma, representing a measure of lesion activity (1, 29, 30). Enhancement is reported to occur in almost all new lesions as shown by serial MR imaging of patients with relapsing-remitting and secondary-progressive MS and lasts about 4 to 6 weeks in most cases (31–33).

Pathologic examination of MS lesions has shown a correlation between the histologic characteristics of lesions and the type of MR contrast enhancement (1, 2). HELs have perivascular inflammation with some myelin loss. NELs have scarring from fibrous astroglial response with minimal inflammation and almost complete myelin loss. RELs, which have an enhancing rim and a nonenhancing center, have peripheral inflammation and complete central demyelination. MS lesions, which are hypointense on T1-weighted images, are associated with severe tissue destruction and axonal loss (4).

Petrella et al (3) evaluated the MTRs of HELs, RELs, and NELs in MS. The MTRs for HELs (mean, 32.2%; SD, 3.4%) were higher than those for NELs (mean, 29.4%; SD, 4.3%) and RELs (mean, 24.5%; SD, 4.0%). A relationship was found between the MTR and the enhancement pattern in which there was pathologic evidence of decreased myelin. HELs, which had the highest MTR, represent lesions with active inflammation and breakdown of the BBB with a greater degree of myelin preservation. In contrast, NELs and the central portion of RELs, which have lower MTRs, have a greater degree of myelin loss. It was important to evaluate the central nonenhancing portion of the REL, as it has been shown that demy-

elination probably occurs centrifugally, with the center of the lesion being the most demyelinated (34). This observation is supported by the fact that the MTR increases from the center to the periphery in an REL (35).

Petrella et al (3) speculated that there may be a pattern of evolution in the enhancement in MS lesions depending on the degree of inflammation and demyelination. An HEL, which is probably an early active inflammatory lesion, may evolve into an REL or NEL. An REL may become an NEL as the peripheral enhancing portion of the REL deactivates. An NEL may become reactivated into an REL but typically not into an HEL, since the center of the lesion is probably the most demyelinated and devascularized. If the NEL becomes completely demyelinated, it may remain burned out and not return to an enhancing pattern.

Diffusion-weighted MR imaging enables evaluation of the random motion of water on a molecular level (5–7). The ADC is a rotationally invariant measurement of the amount of total diffusion within a tissue (7, 12, 13, 16, 25, 26). Trace ADC reflects the structural properties of the cellular compartments of the tissue studied (7). The *in vivo* cellular environment contains cell membranes that form a restrictive barrier to water diffusion. Model systems have been studied that suggest that the axonal cell membrane is sufficient to account for most of the restriction of water diffusion in white matter (8, 36, 37). Diffusion is much more restricted perpendicular to the axis of the axon, where there may be interactions with the myelin sheath, than in a direction parallel to the axon (10, 13–17). The ADC of white matter for the different directions reflects this restrictive property of the tissue. It is not surprising that any process that disrupts the myelination of axons in white matter would also change the diffusion characteristics of water in this tissue.

Interest in studying MS with diffusion-weighted MR imaging has been increasing (18–23). Larsson et al (20) showed that the ratios of diffusion coefficients of MS lesions to NAWM were higher in newer plaques (less than 3 months old, as determined from previous examinations) than in older lesions (more than 3 months old). In that study, only the ratios were presented, because the actual measurement of diffusion coefficients was limited by motion artifacts. Follow-up work by Christiansen et al (21) showed that the ADC data for 39 plaques more than 4 months old (mean, $1.35 \times$

$10^{-9} \text{ m}^2\text{s}^{-1}$) were significantly higher ($P < .01$) than those for NAWM (mean, $0.77 \times 10^{-9} \text{ m}^2\text{s}^{-1}$). Two acute MS lesions, which were approximately 14 days old, also had elevated ADC (mean, $1.99 \times 10^{-9} \text{ m}^2\text{s}^{-1}$). The ADC of NAWM in MS patients was significantly higher than the ADC of NWM in healthy volunteers (21). Heide et al (38) reported increased ADC in lesions detected in experimental allergic encephalomyelitis, which is an animal model of MS. Horsfield et al (18) found that trace ADC was increased in all MS lesions and that ADC was elevated in NAWM in patients with a benign disease course. There was no relationship between ADC and extent of disability in MS patients (18). It has been hypothesized that the elevation in ADC in an MS lesion is related to an increase in the extracellular space within the white matter stemming from the disruption of the axons caused by the demyelinating process and edema (18–21). The cellular environment of the axons probably becomes less restrictive as demyelination evolves. This hypothesis is supported by the significant reduction in anisotropy seen in chronic MS lesions and in the core of acute MS lesions (23). Gass et al (22) reported decreased ADC at the border of some acute plaques, which they attributed to hypercellularity or cytotoxic edema. This report contains some of the first evidence that there may actually be decreases in ADC associated with an MS lesion. In addition, enhancing lesions were hyperintense relative to white matter on diffusion-weighted images while chronic lesions were isointense (22). It is known that both diffusion and T2 relaxation (T2 shine-through) contribute to the signal on diffusion-weighted images. Gass et al (22) hypothesized that the increased intensity in enhancing lesions on diffusion-weighted images results from T2 relaxation that is not matched by an increase in the diffusion coefficient. The latter would tend to reduce the signal on diffusion-weighted images.

The data from our study reveal differences in trace ADC measurements in HELs, RELs, NELs, and NAWM. All MS lesions (NELs, HELs, and RELs) have significantly higher mean trace ADCs relative to NAWM. The mean trace ADC of HELs is significantly less than that of NELs and RELs. There is no significant difference between the mean trace ADC of RELs and NELs. Previously published data (3) have shown significantly increased MTRs in HELs as compared with RELs, and there was a trend toward increased MTR in HELs relative to NELs. These data support the contention that HELs, which have decreased trace ADC and increased MTR in relation to RELs and NELs, have less parenchymal destruction and less demyelination than do RELs and NELs, as demonstrated in histopathologic studies (1, 2). Although there was a significant difference in the MTR of NELs and RELs, there was no significant difference in the trace ADC between NELs and RELs. This may be due to the fact that the SD in trace ADC and MTR

(3) is higher in RELs and NELs than in HELs, which may reflect the wider variability in tissue heterogeneity associated with RELs and NELs.

The temporal evolution of enhancement in MS lesions was seen in two patients. A HEL became a NEL over a period of 9 months. The trace ADC increased from $7.5 \times 10^{-10} \text{ m}^2\text{s}^{-1}$ to $9.7 \times 10^{-10} \text{ m}^2\text{s}^{-1}$, probably reflecting the subsequent increase in extracellular space with increasing demyelination and decreasing inflammation. A REL became a NEL over a period of 11 months, with trace ADC changing from $2.1 \times 10^{-9} \text{ m}^2\text{s}^{-1}$ in the center of the REL to $1.8 \times 10^{-9} \text{ m}^2\text{s}^{-1}$ in the NEL. These two examples support the dynamic evolution of enhancement in MS lesions, as reported by Petrella et al (3).

Although the mean trace ADC of HELs is significantly higher than that of NAWM, four of 28 HELs had trace ADC values that were 2 SD below the mean for NAWM. None of the RELs or NELs had trace ADC values below 2 SD of the mean of the NAWM. This subset of HELs with a low trace ADC may provide insight into the cellular architecture of these lesions. We postulate that the decrease in ADC of these HELs may be similar to the process in acute ischemia (8, 11) and postanoxic demyelination (39). There may be shifts in intracellular water protons and changes in membrane permeability that lead to decreased ADC. HELs represent active lesions with a predominant inflammatory component (1, 27, 28). The influx of inflammatory cells and associated macromolecules may also lead to restriction of water diffusion and reduction in trace ADC. Perhaps the subset of HELs with a low trace ADC represents the very early enhancing lesion with marked inflammation and no significant demyelination; however, since it is currently not possible to accurately date MS lesions, we cannot classify HELs as either early or late.

It has been suggested that acute MS lesions may have higher ADC values than chronic lesions (18, 20, 21). Larsson et al (20) found that acute lesions less than 3 months old (by review of serial examinations) had higher diffusion coefficient ratios than did chronic lesions. Christiansen et al (21) described two acute plaques that were approximately 14 days old with higher ADCs than chronic lesions, which were more than 4 months old. It is difficult to directly compare these findings with our study, as we made no attempt to ascertain the age of the MS lesions, and the other studies did not characterize the enhancement patterns of the MS lesions. Currently, the trace ADC of a hyperacute MS lesion (less than 24 hours old) is still unknown.

There are important limitations to our study. Only patients with enhancing MS lesions were included in the project. The trace ADC ROIs were not uniform in size, which may have led to increased variability in the SD of the measurements. The largest ROI possible was intentionally used for evaluation of each lesion to reduce the ROI SD and

the statistical noise. The ROIs were selected on the baseline images to eliminate any misregistration errors between the anatomic images and the diffusion-weighted images. Image distortions between the diffusion directional images, however, may have contributed to some partial volume sampling errors within ADC measurements.

Conclusion

A relationship exists between the trace ADC and the pattern of enhancement in MS lesions. There are significant increases in trace ADC in NELs and RELs, in which there is histopathologic evidence of increased myelin loss relative to HELs, which are predominantly inflammatory with more myelin preservation. Diffusion-weighted MR imaging findings and trace ADC measurements offer another perspective on the pathologic heterogeneity of MS lesions.

References

- Katz D, Taubenberger J, Cannella B, McFarlin D, Raine C, McFarland H. **Correlation between magnetic resonance imaging findings and lesion development in chronic, active multiple sclerosis.** *Ann Neurol* 1993;34:661-669
- Nesbit G, Forbes G, Scheithauer B, Okazaki H, Rodriguez M. **Multiple sclerosis: histopathological and MR and/or CT correlation in 37 cases at biopsy and three cases at autopsy.** *Radiology* 1991;180:467-474
- Petrella J, Grossman R, McGowan J, Campbell G, Cohen J. **Multiple sclerosis lesions: relationship between MR enhancement pattern and magnetization transfer effect.** *AJNR Am J Neuroradiol* 1996;17:1041-1049
- vanWalderveen M, Kamphorst W, Scheltens P, et al. **Histopathologic correlate of hypointense lesions on T1-weighted spin-echo MRI in multiple sclerosis.** *Neurology* 1998;50:1282-1288
- Stejskal E, Tanner J. **Spin diffusion measurements: spin echoes in the presence of a time-dependent field gradient.** *J Chem Phys* 1965;42:288-292
- LeBihan D, Breton E, Aubin M. **MR imaging of intravoxel incoherent motions: application to diffusion and perfusion in neurologic disorders.** *Radiology* 1986;161:401-407
- LeBihan D. **Separation of diffusion and perfusion in intravoxel incoherent motion (IVIM) MR imaging.** *Radiology* 1988;168:497-505
- Moseley M, Kucharczyk J. **Diffusion in brain ischemia.** In: LeBihan D, ed. *Diffusion and Perfusion Magnetic Resonance Imaging*. New York: Raven;1995:159-167
- Moseley M, deCrespigny A, Roberts T, Kozniowska E, Kucharczyk J. **Early detection of regional cerebral ischemia using high-speed MRI.** *Stroke* 1993;24:160-165
- Moseley M, Kucharczyk J, Mintorovitch J, et al. **Diffusion-weighted MR imaging of acute stroke: correlation with T2-weighted and magnetic susceptibility-enhanced MR imaging in cats.** *AJNR Am J Neuroradiol* 1990;11:423-432
- Moseley M, Cohen Y, Mintorovitch J, et al. **Early detection of regional cerebral ischemia in cats: comparison of diffusion and T2-weighted MRI and spectroscopy.** *Magn Reson Med* 1990;14:330-346
- Warach S, Chien D, Li W, Ronthal M, Edelman R. **Fast magnetic resonance diffusion-weighted imaging of acute human stroke.** *Neurology* 1992;42:1717-1723
- Basser P, Pierpaoli C. **Microstructural and physiological features of tissues elucidated by quantitative-diffusion-tensor MRI.** *J Magn Reson B* 1996;111:209-210
- Conturo T, McKinstry R, Aronovitch J, Neil J. **Diffusion MRI: precision, accuracy and flow effects.** *NMR Biomed* 1995;8:307-332
- LeBihan D. **Molecular diffusion, tissue microdynamics and microstructure.** *NMR Biomed* 1995;8:375-386
- Pierpaoli C, Jezzard P, Basser P, Barnett A, Dichiro G. **Diffusion tensor imaging of the human brain.** *Radiology* 1996;201:637-648
- vanGelderden P, deVleeschouwer M, DesPres D, Pekar J, vanZijl P, Moonen C. **Water diffusion and acute stroke.** *Magn Reson Med* 1994;31:154-163
- Horsfield M, Lai M, Webb S, et al. **Apparent diffusion coefficients in benign and secondary progressive multiple sclerosis by nuclear magnetic resonance.** *Magn Reson Med* 1996;36:393-400
- Horsfield M, Larsson H, Jones D, Gass A. **Diffusion magnetic resonance imaging in multiple sclerosis.** *J Neurol Neurosurg Psychiatry* 1998;64(Suppl 1):S80-S84
- Larsson H, Thomsen C, Frederiksen J, Stubgaard M, Henriksen O. **In vivo magnetic resonance diffusion measurement in the brain of patients with multiple sclerosis.** *Magn Reson Imaging* 1992;10:7-12
- Christiansen P, Gideon P, Thomsen C, Stubgaard M, Henriksen O, Larsson H. **Increased water self-diffusion in chronic plaques and in apparently normal white matter in patients with multiple sclerosis.** *Acta Neurol Scand* 1993;193:195-199
- Gass A, Gaa J, Schreiber W, et al. **Echo planar diffusion weighted magnetic resonance imaging in patients with active multiple sclerosis.** In: *Book of Abstracts: International Society of Magnetic Resonance in Medicine, Vancouver, Canada, 1997*. International Society of Magnetic Resonance in Medicine; 1997:658
- Tievsky A, Ptak T, Wu O, et al. **Evaluation of MS lesions with full tensor diffusion-weighted imaging and anisotropy mapping.** In: *Book of Abstracts: International Society of Magnetic Resonance in Medicine, Vancouver, Canada, 1997*. International Society of Magnetic Resonance in Medicine; 1997:666
- Poser C, Paty D, Scheinberg L. **New diagnostic criteria for multiple sclerosis: guidelines for research protocols.** *Ann Neurol* 1983;13:227-231
- Basser P, Pierpaoli C. **A simplified method to measure the diffusion tensor from seven MR images.** *Magn Reson Med* 1998;39:928-934
- Rowley H, Grant P, Roberts T. **Diffusion MR imaging.** *Neuroimaging Clin North Am* 1999;9:343-361
- McFarland H. **The lesion in multiple sclerosis: clinical, pathological, and magnetic resonance imaging considerations.** *J Neurol Neurosurg Psychiatry* 1998;64(Suppl 1):S26-S30
- McDonald W. **Rachelle Fishman-Matthew Moore lecture: the pathological and clinical dynamics of multiple sclerosis.** *J Neuropathol Exp Neurol* 1994;53:338-343
- Grossman R, Gonzalez-Scarano F, Atlas S, Galetta S, Silberberg D. **Multiple sclerosis: gadolinium enhancement in MR imaging.** *Radiology* 1986;161:721-725
- McDonald W. **The dynamics of multiple sclerosis.** *J Neurol* 1993;240:28-36
- Miller D, Albert P, Barkof F, et al. **Guidelines for the use of magnetic resonance techniques in monitoring the treatment of multiple sclerosis.** *Ann Neurol* 1996;39:6-16
- Thompson A, Kermode A, Wicks D, et al. **Major differences in the dynamics of primary and progressive multiple sclerosis.** *Ann Neurol* 1991;29:53-62
- Thompson A, Miller D, Youl B, et al. **Serial gadolinium enhanced MRI in relapsing/remitting multiple sclerosis of varying disease duration.** *Neurology* 1992;42:60-63
- Dousset V, Grossman R, Ramer K, et al. **Experimental allergic encephalomyelitis and multiple sclerosis: lesion characterization with magnetization transfer imaging.** *Radiology* 1992;182:483-491
- Hiehle J, Grossman R, Kramer K, Gonzalez-Scarano F, Cohen J. **Magnetization transfer effects in MR-detected multiple sclerosis lesions: comparison of gadolinium-enhanced spin-echo images and non-enhanced T1-weighted images.** *AJNR Am J Neuroradiol* 1995;16:69-77
- Beaulieu C, Allen P. **Water diffusion in the giant axon of the squid: implications for diffusion-weighted MRI of the nervous system.** *Magn Reson Med* 1994;32:579-583
- Beaulieu C, Allen P. **Determinants of anisotropic water diffusion in nerves.** *Magn Reson Med* 1994;31:394-400
- Heide A, Richards T, Alvord E, Peterson J, Rose L. **Diffusion imaging of experimental allergic encephalomyelitis.** *Magn Reson Med* 1993;29:478-484
- Roychowdhury S, Maldjian J, Galetta S, Grossman R. **Postanoxic encephalopathy: diffusion MR findings.** *J Comput Assist Tomogr* 1998;22:992-994